HELICOPTER FUSELAGE VIBRATIONS INDUCED BY THE ROTOR

Didier Petot, Marc Rapin
Onera
Châtillon, France

ABSTRACT

A methodology is developed for predicting the vibratory behaviour of a complete helicopter by coupling a full aeroelastic rotor code with fuselage modes. Applications are made on a simplified helicopter. Aircraft vibratory characteristics are evaluated as a function of blade and fuselage stiffness and the effect of fuselage excitation on blade loads is calculated.

A first attempt is made at reducing vibration levels by tuning the fuselage modes through an optimisation procedure. Encouraging results show the feasibility of the approach and call for further research.

1. INTRODUCTION

Over the past few years the ONERA's fully aeroelastic rotor code [5] has been successully validated against a number of data bases. Its reliability now allows the study of the in-flight vibrations of a complete helicopter. A methodology for this is developed by coupling the code with fuselage modes.

For a simple but realistic application, a hypothetical helicopter is chosen closely resembling a 2 ton aircraft. The fuselage is simplified and defined by beam type finite elements. Flight conditions considered are hover and forward flight at an advancd ratio of 0.34.

In order to evaluate the influence of the different vibratory motions, overall aircraft vibration characteristics are calculated step by step for increasingly complex configurations going from stiff blades on a fixed hub to soft blades on a flexible fuselage. The effect of fuselage excitation on unsteady blade loads is also considered. It is shown that induced stress levels may not be negligible.

The ultimate objective of this ongoing research programme is not merely to predict vibration levels but also to reduce them. A minimisation procedure is developed anf first attemps are made at reducing pilot's seat vibrations through tuning fuselage modes. These give very encouraging results and show the feasibility of the approach.

2. THE HELICOPTER CODE

2.1 Conventional reference frame

The helicopter is placed in a galilean reference frame having the x axis forward, the y axis to the left and the z axis upward.

2.2 Kinematics

The ONERA aeroelastic helicopter code [5] is based on a set of routines that calculate the contribution of a blade element *dm* to the global equations of a rotor. The blade is cantilevered at the end of a series of transformations that connect the blade root to the general galilean frame. These transformations completely describe the aircraft studied. They can be translations or rotations and can be considered as degrees of freedom or not. A special transformation is used to branch the series of transformations in order to account for the n blades. The blades can be flexible, their deformation being then projected on a modal base. Fig 1 describes the system.

Many types of structure can thus be taken into account: rotors mounted on an tilting body,

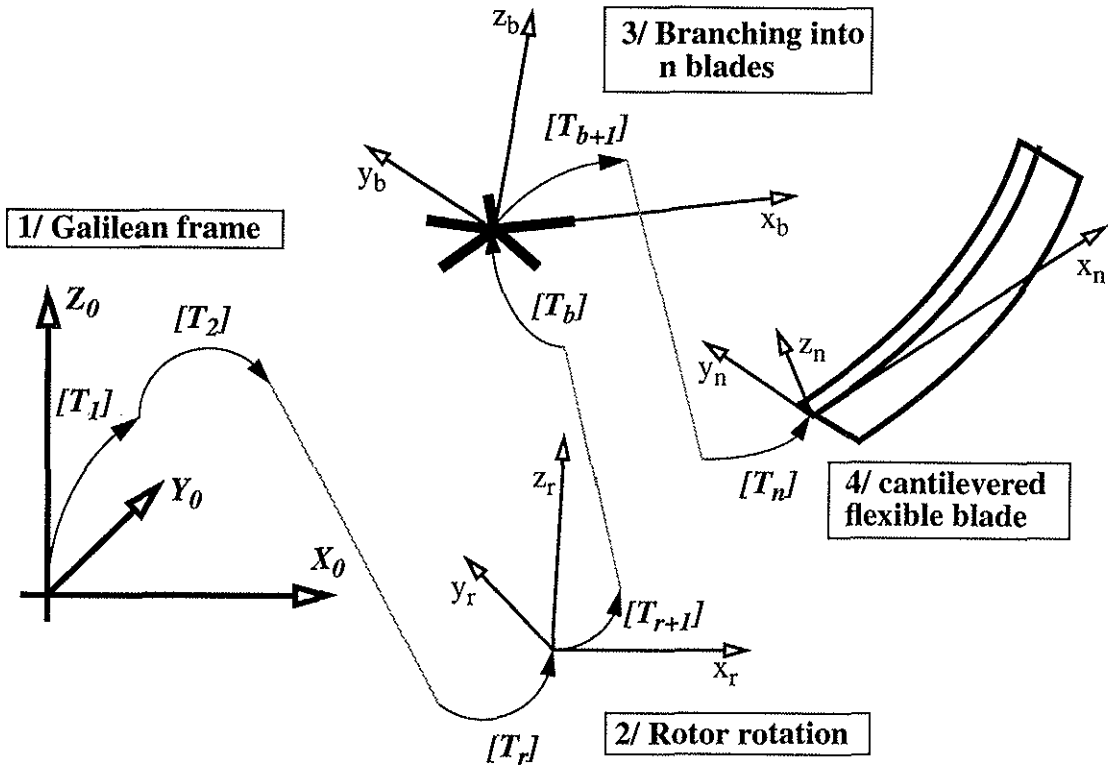

Fig 1: Definition of the studied structure in ONERA helicopter code

guimbaled rotors (teetered rotors, universal joints) or the classical hinged rotor. A projection of the equations on a body modal bases is then made, which accounts for all body deformations.

2.3 Equations

The equations are written in the general form:

$$M_{st} \cdot \ddot{q} + B_{st} \cdot q' + K_{st} \cdot q = F_{st} + F_{ae}$$

where the subscript *st* stands for «structural» and the subscript *ae* for «aerodynamic». The equations thus obtained can then be used for several purposes: calculation of a periodic response, time integration or stability.

2.4 Aerodynamics

Quasi-steady aerodynamics can be completed by a linear unsteady option developed at ONERA, as well as by two dynamic stall options [1 and 2].

Aerodynamic damping and stiffness matrices can also be calculated but only with the quasi-steady or linear unsteady options.

2.5 Induced velocities

The main induced velocity flow fields available are those of MEIJER-DREES and METAR [4]. METAR which describes a prescribed wake requires more CPU time and is not available for all the options, but naturally it yields the better results.

2.6 Stability

The equations are linearized around a certain trim and are completed by the aerodynamic damping and stiffness matrices. Stability is given by the eigen values of :

$$M_{st} \cdot \ddot{q} + (B_{st} + B_{ae}) \cdot \dot{q} + (K_{st} + K_{ae}) \cdot q = 0$$

An option is also available for stability in forward flight using the Floquet analysis. The equation is integrated simultaneously over a rotor

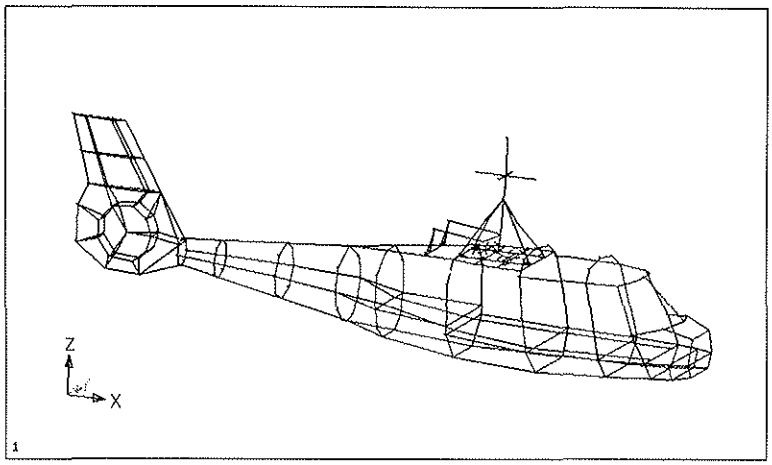

Fig 2: Finite element model of the fuselage

revolution, followed by a treatment of the response.

2.7 Periodic response

The variables are assumed to be periodic and are expressed through Fourier series the coefficients of which become the unknowns of the problem. The solution is then obtained using a mathematical algorithm (HYBRD) that searches for the roots of a set of non-linear equations of :

$$\boldsymbol{M}_{st} \cdot \ddot{q} + \boldsymbol{B}_{st} \cdot q' + \boldsymbol{K}_{st} \cdot q = \boldsymbol{F}_{st} + \boldsymbol{F}_{ae}$$

Additional equations can be added to this set, in order to account for control laws, aircraft trim, etc.

For the in-flight rotor-fuselage coupling, an additional feature had to be developed. In this case, the fuselage vibration has to take into account the 6 rigid body displacements. As a simple displacement of the aircraft does not change its operating conditions, the mathematical procedure cannot find a value for it.

Artificial constraints had to be introduced in order to keep the aircraft in its mean position. These constraints restitute the forces and moments required to maintain this position. They represent the weight of the aircraft, the aerodynamic forces on the fuselage and on the tail and the action of the tail rotor.

Calculations are usually performed considering the variables from one blade only, assuming that the other blades have exactly the same behaviour. Nevertheless, a true multi-blade calculation is possible and even necessary in the case of an asymmetric hub such as a teetered rotors.

2.8 Time integration

The same set of equations can be solved step by step using a mathematical tool (HPCG, but an option with LSODI also exists). In this case, the calculation has to be performed without external trim. This option can show the effect of a perturbation on the aircraft (turbulence, manoeuvres, etc).

2.9 Optimisation

An optimisation tool for the rotor has also been developed. It minimises a choosen penalty using the classical mathematical procedure CONMIN, each CONMIN iteration being a periodic response calculation.

2.10 Exportation of the equations

The calculated equations can be saved and used outside the code. This has allowed the calculation of the vibration of an aircraft subjected to a random external excitation which will be pre-

Table 1: Free modes of the fuselage with no rotor

Mode	Freq (Hz)	Damp.	Mass (m^2Kg)	Displacement at the hub centre					
				x (m) forw'd	y (m) leftw'd	z (m) upw'd	Rot x (Rd)	Rot y (Rd)	Rot z (Rd)
Transl.before	0.000	0.	1928.	1.	0.	0.	0.	0.	0.
Transl.left	0.000	0.	1928.	0.	1.	0.	0.	0.	0.
Transl.above	0.000	0.	1928.	0.	0.	1.	0.	0.	0.
Roll	0.000	0.	1607.	0.	-1.77	0.	1.	0.	0.
Pitch	0.000	0.	4784.	1.77	0.	0.	0.	1.	0.
Yaw	0.000	0.	4052.	0.	0.	0.	0.	0.	1.
Lateral.1	8.40	0.02	10000.	0.0125	-0.4179	0.0005	0.0436	0.0098	0.1193
Vertical.1	13.22	0.02	10000.	1.1976	-0.0006	0.3063	0.0010	1.7822	-0.0148
Torsion.1	14.65	0.02	10000.	0.0979	0.7825	-0.0446	0.2314	0.0681	-0.1696
Lateral.2	18.04	0.02	10000.	0.2932	0.7147	-0.1045	-2.1695	0.2094	-4.5596
Vertical.2a	19.07	0.02	10000.	3.6073	1.6445	-1.0423	-1.2253	2.5231	1.2620
Vertical.2b	19.16	0.02	10000.	5.8726	-0.8008	-1.6908	0.5903	4.1175	-0.6128
Tail.Vertical.1	21.09	0.02	10000.	1.5160	0.1454	0.0911	-0.1359	1.1482	0.0417
Mast.Roll	23.40	0.02	10000.	-0.1559	5.9723	0.0609	-6.1019	-0.1052	0.3599
Lateral.3	24.73	0.02	10000.	0.0070	0.8641	-0.0335	-0.6966	0.0429	1.0774
Opp.Tail/Mast	25.05	0.02	10000.	0.5915	-0.0511	-0.8189	0.0454	1.2587	-0.0508
Vertical.3	30.82	0.02	10000.	1.7511	0.2191	1.1766	-0.2019	1.1480	-0.0333
Lateral.Cabin	32.79	0.02	10000.	-0.1051	4.8249	-0.0733	-4.6207	0.0107	-0.3950

sented later.

The equations have also been coupled with a fixed wing aeroelastic stability code leading to the prediction of the dynamic behaviour of a complete tilt rotor aircraft.

3. THE AIRCRAFT AND FLIGHT CONDITIONS

The present study was conducted on a hypothetical helicopter that possesses all the characteristics of a classical medium size aircraft, with a total mass of 2164 kg.

3.1 Rotor

The rotor is made of three hinged straight blades that are 5.25 meters long, flexible and dynamically defined by their first 7 non-rotating cantilevered modes. Their chord is 0.35m.

Their rotating frequencies are 2.43 and 30.6 Hz for the first and second lead-lag modes, 6.62, 17.38 and 29.43 Hz for the first, second and third flapping moides and 27.3 Hz for the torsion mode.

The rotation speed of the rotor is 6.45 Hz.

3.2 Fuselage

The fuselage is modeled by beam elements that were developed at ONERA in order to reproduce correctly the low frequency behaviour of a real helicopter [3]. It is made up of 234 nodes, 562 beams and 1390 degrees of freedom. Its geometry is shown in fig 2.

No fuselage or tail aerodynamics are taken into account except for the total drag.

The fuselage modes are calculated using the NASTRAN finite element code and neglecting the rotor. This simplification is introduced be-

Table 2: Complete helicopter natural frequencies in-flight

Modal characteristics (body modes shaded)	Name	Hover				Forward flight, V=72 m/s	
		Snapshot eig. Fq(Hz) / Damp.		Floquet analysis Fq (Hz) / Damp.		Snapshot eigenvalues Freq (Hz) / Damping	
Blade lead-lag x 3	ll'_1	2.56	0.008	Ω - 2.56	0.005	2.53 --> 2.54	0.008 --> 0.010
	ll_1	2.71	0.006	2.71	0.006	2.70	0.009
	ll''_1	3.22	0.007	2.70 + Ω	0.004	3.21 --> 3.25	0. --> 0.016
Blade flapping x 3	f'_1	6.49	0.310	6.63 - Ω	6.91	5.55 --> 6.03	0.21 --> 0.38
	f_1	6.63	0.287	6.63	0.287	6.48 --> 6.80	0.14 --> 0.27
	f''_1	6.49	0.291	6.47 + Ω	0.154	7.24 --> 7.64	0.22 --> 0.30
Lateral 1	F_1	8.39	0.020	8.37	0.002	8.39	0.020
Vertical 1	F_2	12.87	0.019	13.02	0.019	12.85 --> 12.87	0.018 --> 0.020
Torsion + Vertical 2b	F_3	14.39	0.019	14.47	0.019	14.36 --> 14.39	0.018 --> 0.019
Torsion 1	F_4	14.62	0.019	14.84	0.0019	14.61 --> 14.63	0.019
Lateral 2 + Body roll	F_5	17.50	0.019	17.68	0.018	17.49 --> 18.53	0.018 --> 0.021
2nd blade flapping x 3	f'_2	17.73	0.078	17.71 - Ω	0.124	17.19 --> 17.36	0.101 --> 0.140
	f_2	17.98	0.075	17.98	0.074	17.76 --> 18.23	0.037 --> 0.100
	f''_2	17.75	0.079	17.75 + Ω	0.058	17.47 --> 17.63	0.057 --> 0.124
Vert 2a + Lateral 2	F_6	18.24	0.019	18.28	0.019	18.25 --> 18.26	0.019
Mast Roll	F_7	20.07	0.019	20.13	0.019	20.08	0.019
Tail.Vertical 1	F_8	21.01	0.020	21.01	0.020	21.01	0.020
Lateral.3	F_9	24.69	0.020	24.69	0.020	24.69	0.020
Opposition Tail/Mast	F_{10}	24.95	0.021	24.95	0.021	24.94	0.021
Blade torsion x 3	t'	26.14	0.194	26.13 - Ω	0.255	26.97 --> 27.36	0.094 --> 0.107
	t	26.18	0.196	26.18	0.196	27.32 --> 27.80	0.110 --> 0.127
	t"	26.15	0.192	26.14 + Ω	0.156	27.79 --> 28.32	0.110 --> 0.217
3rd blade flapping x 3	f'_3	29.43	0.087	29.46 - Ω	0.111	29.17 --> 29.21	0.066 --> 0.171
	f_3	29.41	0.068	29.42	0.070	29.31 --> 29.67	0.042 --> 0.135
	f''_3	29.45	0.087	29.43 + Ω	0.071	Undecidable	Undecidable
Lateral Cabin	F_{11}	30.27	0.014	30.72	0.017	30.24 --> 30.27	0.014 --> 0.015
Vertical 3	F_{12}	30.52	0.035	30.60	0.035	30.57 --> 30.68	0.026 --> 0.030
2nd blade lead-lagx 3	ll'_2	31.02	0.008	30.90-Ω	0.007	31.00 --> 31.09	0.007 --> 0.009
	ll_2	30.86	0.003	30.87	0.006	30.86 --> 30.87	0.003 --> 0.004
	ll''_2	31.87	0.004	31.46+Ω	0.004	31.76 --> 31.92	0.008 --> 0.009

cause the blade mass is not easily accounted for through the hinges.

The calculated modes are listed in table 1. Three modes were found in the vicinity of 3Ω (19.35 Hz) which is the frequency of excitation by the rotor. It will be shown later that considering each blade individually by branching the rotor will shift these frequencies.

The first 12 modes were retained for this study (up to 5Ω), in addition to the 6 rigid body modes. It is difficult to give these modes descriptive names. If one thinks of the helicopter as a simple beam, one might expect basic modes such as sets of vertical bending (first, second, third...), lateral bending and fuselage torsion modes. In fact the finite element calculation reveals several modes sharing the same basic deflection pattern.

For the sake of clarity, the first 4 non-rigid modes were defined as Lateral.1, Vertical.1, Torsion.1, Lateral.2. The next 3 modes have the same basic deflexions and were named Vertical.2a, Vertical.2b and VertTail.1, since for the last of these the tail movement is predominant. The next mode has a rolling motion of the rotor-shaft followed by a Lateral.3 mode. The following mode has the shaft and the tail moving in counter phase. The last modes kept are a Vertical.3 mode and a lateral mode in which only the cabin seems to move.

For the calculations, 2% of damping was assumed for each flexural mode.

3.3 Flight conditions

The helicopter cruises at 72 m/s which corresponds to an advance ratio of μ=0.34. At this speed, the pitch attitude of the aircraft is taken as 9 degrees nose-down.

The aircraft is force trimmed, that is to say that the thrust of the rotor balances its weight and creates a propulsive force of C_T/σ=0.100. A zero lateral force is assumed.

Calculations were carried out with quasi-steady aerodynamics including a linear unsteady component. The METAR prescribed wake was used.

4. CALCULATING THE AIRCRAFT MODES

4.1 Introduction

The aircraft has 18 degrees of freedom for the fuselage and 27 for the rotor (7 blade flexural modes plus flapping and lead-lag, for each of 3 blades). Forty-five modes are thus expected to be found, the first 30 of these are given in table 2. Calculations were performed in hover, with zero pitch attitude, and in forward flight.

The modal characteristics of a complete aircraft are not obvious to obtain. Periodic coefficients are present in the forward flight equations, but in fact, these already exist in hover because of the mixture of the degrees of freedom rotating on the rotor and those that are on the fuselage.

In the presence of periodic coefficients, the FLOQUET theory is necessary to obtain generalized modes. This method requires much computing power and leads to results often difficult to analyse.

A procedure has been suggested [8] where the eigenvalues of the instantaneous equation at each azimuth are determined. This is known as the snapshot eigenvalue method.

4.2 Snapshot eigenvalues in hover

The frequencies and damping obtained for the first 30 modes of the helicopter model are shown in table 2. Body modes are shaded and blade modes occur in groups of 3 close frequencies.

This last point can be understood if one remembers that the rotor is supposed fixed at some azimuthal position (rotational effects still being taken into account). For each blade mode, the coupling with fuselage degrees of freedom slightly shifts each of the triple rotor frequencies, which then become distinct. Blade flapping, for example, would lead to one rotor mode coupled with the vertical vibration of the fuselage, a second with pitch and a third with roll.

In the case of hovering flight, the symmetry of the rotor causes the frequencies and dampings not to depend on azimuth although the equations have periodic coefficients. On the other hand, the mode shapes vary with the azimuth angle.

Calculations show the body mode frequencies and shapes close to those of the isolated fuselage, although some of the couplings are difficult to understand. There is also little change in the damping.

Each blade mode branches into 3 as expected. This effect is quite large in lead-lag. Lead-lag damping is quite low and flapping is heavely damped, as expected. Torsion damping is also high due to unsteady aerodynamics.

Table 3: Vibration at an advance ratio of 0.34

Table 3a

Configuration	θ	θc	θs	Power
Stiff blades, cantilevered rotor	0.32°	0.62°	-1.61°	248 kW
Flexible blades, cantilevered rotor	1.53°	0.24°	-1.77°	246 kW
Flexible blades, stiff fuselage	1.53°	0.24°	-1.77°	246 kW
Flexible blades, flexible fuselage	1.51°	0.24°	-1.77°	248 kW

Table 3b

Configuration	Forces and moments at the hub				
	Fx (3Ω)	Fy (3Ω)	Fz (3Ω)	Rot Mt (2Ω)	Mt link(2Ω)
Stiff blades, fixed hub	329 N	376 N	546 N	927 mN	225 mN
Flexible blades, fixed hub	422 N	103 N	3271 N	575 mN	170 mN
Flexible blades, stiff fuselage	365 N	72 N	3214 N	237 mN	169 mN
Flexible blades, flexible fuselage	845 N	332 N	3173 N	235 mN	167 mN
Optimisation of Γz pilot's seat	890 N	536 N	3193 N	241 mN	169 mN
Optimisation of Γ pilot's seat	761 N	795 N	3163 N	229 mN	164 mN

Table 3c

Configuration	Maximum stress at the blade root				
	Chordwise shear	Vertical shear	Torsion moment	Flapping moment	Lead-lag moment
Stiff blades, fixed hub	317 N	-781 N	-124 mN	-946 mN	-925 mN
Flexible blades, fixed hub	159 N	221 N	-112 mN	-510 mN	-890 mN
Flexible blades, stiff fuselage	163 N	217 N	-113 mN	-508 mN	-887 mN
Flexible blades, flexible fuselage	184 N	220 N	-113 mN	-538 mN	-917 mN
Optimisation of Γz pilot's seat	176 N	226 N	-114 mN	-553 mN	-952 mN
Optimisation of Γ pilot's seat	225 N	216 N	-113 mN	-518 mN	-977 mN

Table 3d

Configuration	Acceleration at the pilot's seat				
	Γx / forw'd	Γy / left	Γz / upw'd	dΓz/dx	dΓz/dy
Flexible blades, stiff fuselage	0.06 m/s^2	0.24 m/s^2	1.32 m/s^2	0.16 Rd/s^2	0.16 Rd/s^2
Flexible blades, flexible fuselage	1.13 m/s^2	1.75 m/s^2	0.77 m/s^2	3.16 Rd/s^2	1.07 Rd/s^2
Optimisation of Γz pilot's seat	1.22 m/s^2	1.76 m/s^2	0.12 m/s^2	3.17 Rd/s^2	1.06 Rd/s^2
Optimisation of Γ pilot's seat	0.11 m/s^2	0.24 m/s^2	0.20 m/s^2	0.29 Rd/s^2	0.58 Rd/s^2

4.3 Floquet analysis in hover

In the case of a symmetrical rotor (more than 2 blades in hover), the use of multiblade coordinates removes the periodic coefficients. This change of variables plays the role of a Floquet analysis.

The modes obtained using the multiblade coordinates are now true modes for the fuselage degrees of freedom.

The rotor modes are still found by groups of three: a collective (frequency ω), a regressive (at about ω-Ω, Ω=6.45 Hz) and a progressive (about ω+Ω) mode. The shift in frequency obtained is due to the fact that the vibration is considered in the fuselage fixed reference frame.

In order to evaluate the snapshot eigenvalue method, one must first make the appropriate shift in the frequencies of the blade modes and then compare the dampings expressed in s^{-1} and not in non-dimensional form as given here.

This manipulation is not very satisfactory, but it can be seen that the modes obtained are quite close to those given by the snapshot eigenvalue method, both in frequency and in damping. Thus, the snapshot eigenvalue method is usefuly reliable. Some differences can nevertheless be noticed, especially relative to the lowest frequency blade flapping and lead-lag modes.

4.4 Snapshot eigenvalue in forward flight

Because of the periodic aerodynamic environment, the frequencies and damping calculated at each azimuth now fluctuate. Their range of values is shown in table 2.

The blade modes show quite large oscillations. Nevertheless, the average value of their damping remains of the same order as in the case of hover.

The results obtained in hover are thus reasonably reliable for forward flight. The biggest differences with hovering conditions being the shift in frequency of two of the blade first flapping frequencies and the increase in the torsional frequencies which are not understood.

4.5 Floquet analysis in forward flight

The use of multiblade coordinates is not sufficient to suppress the periodic coefficients caused by the aerodynamics. A true Floquet analysis has to be performed. This has been attempted but the difficulties in time integration with the 6 zero frequency modes of the aircraft (some stiffness had to be introduced) and the complexity of the response have not yet been resolved.

The snapshot eigenvalue method is therefore the only available tool at present.

5. VIBRATION OF THE AIRCRAFT

5.1 Characteristic behaviour

The general vibration of the aircraft in forward flight (72 m/s) has been studied for conditions, where the number of degrees of freedom is increased step by step.

Tables 3 summarize the results. There are 3 components in 3Ω of the forces at the hub centre in the x-axis, the 2Ω component of the rotor rotating moment, the moment at the pitch link (table 3b) and the resulting acceleration at the pilot's seat (table 3d). The maximum stresses during a cycle, at the blade root, is also shown (table 3c).

Fixed Hub : The results show that the stiff blade calculations lead to the larger hub loads, except for the vertical force component at the hub centre (table 3b). This shows that blade softness generally reduces hub loads.

In fact, the helicopter with soft blades flies with different pitch controls (table 3a) because the blade torsion (dynamically) changes the aerodynamic angle of attack.

Stiff fuselage : Allowing the rigid body movements of a stiff fuselage further reduces the forces at the hub centre, by 20 to 50%.

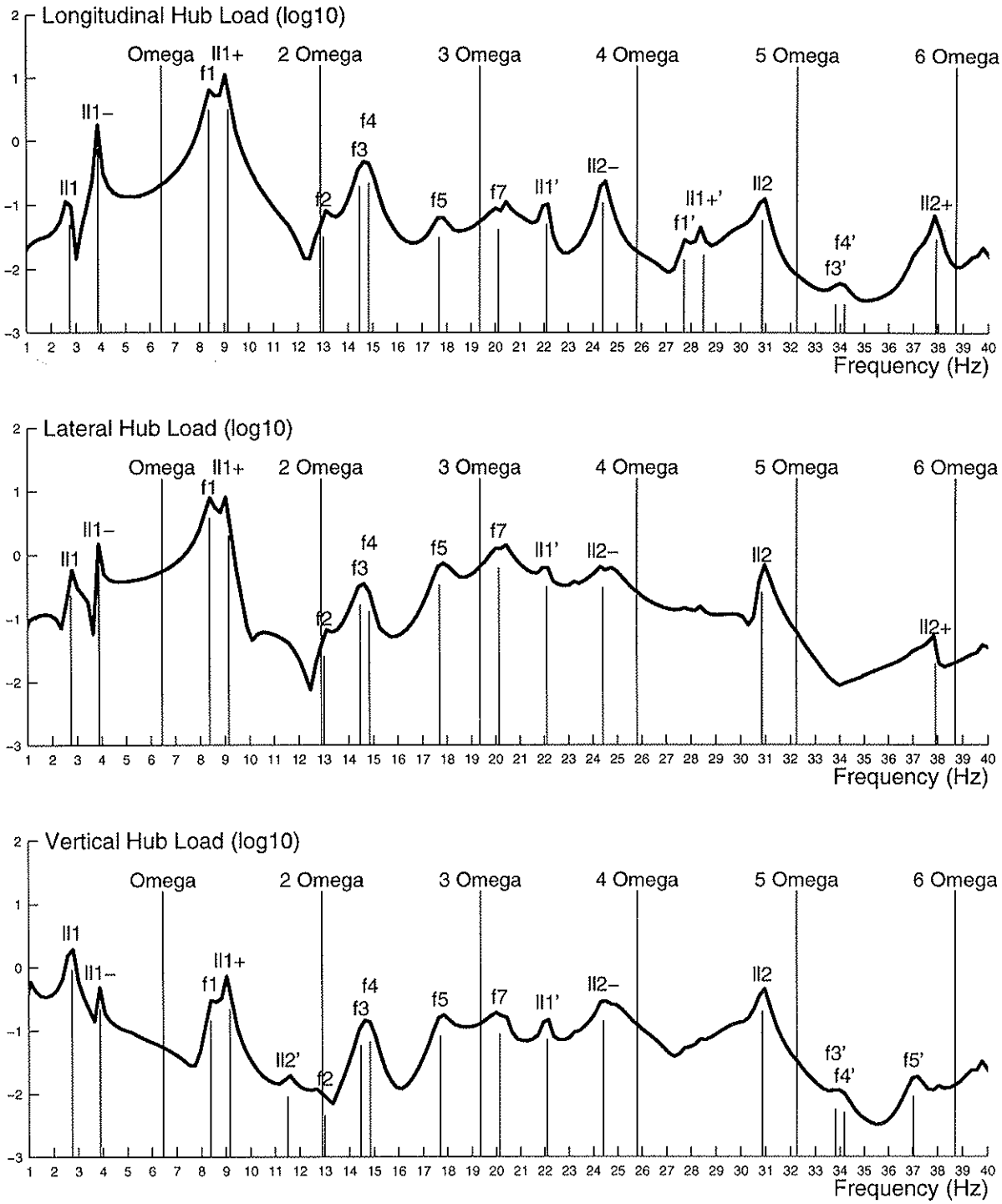

Fig 3: Response to a white noise excitation of the helicopter fin.

Table 4: Optimised fuselage frequencies

Fuselage modes		Original frequencies	Optimisation Acc. z pilot	Optimisation Acc. pilot
Lateral.1	7	8.40 Hz	8.40 Hz	10.09 Hz
Vertical.1	8	13.22	13.36	12.54
Torsion.1	9	14.65	14.85	12.86
Lateral.2	10	18.04	18.28	14.43
Vertical.2a	11	19.07	20.11	15.26
Vertical.2b	12	19.16	19.71	15.33
Tail.Vertical.1	13	21.09	20.78	25.31
Mast.Roll	14	23.40	22.55	28.00
Lateral.3	15	24.73	24.73	19.78
Opp.Tail/Mast	16	25.05	25.06	30.05
Vertical.3	17	30.82	30.82	24.65
Lateral.Cabin	18	32.79	32.80	26.23

Flexible fuselage : Taking into account the flexure modes of the fuselage increases the stresses to levels exceeding those of the fixed hub (table 3c). The dynamics of the fuselage do not act in the right direction here. The fact that the lateral rather than the vertical accelerations at the pilot's seat are increased shows that the main problem originates from the rotating moment on the hub, rather than the vertical effort.

The larger amplitude of vibration of the fuselage logically comes from the f_5, f_6, f_7 and f_8 modes whose frequencies are in the neighbourhood of the excitation at 3Ω.

5.2 Forced response

Sinusoidal excitation : A sinusoidal excitation was applied to the fuselage in order to check its vibration sensitivity. The excitation was applied sideways on the helicopter fin and could simulate an aerodynamic excitation.

The generalized force generated by this excitation was introduced into the right hand side of the general equations of the system:

$$\boldsymbol{M}_{st} \cdot \ddot{q} + \boldsymbol{B}_{st+ae} \cdot \dot{q} + \boldsymbol{K}_{st+ae} \cdot q = \frac{\partial W_{ext}}{\partial q}$$

in which, it must be remembered, all the matrices have the periodicity Ω.

If the excitation frequency of the tail is ω, it is assume that the vibration of the aircraft can be written in the general form:

$$q = \sum_{i=1}^{n} \sum_{k=-k_{max}}^{k_{max}} q_{ik} \cdot \cos\left((\omega + k\Omega)\, t + \phi_k \right)$$

If the highest frequencies are neglected (that is, the highest values of k), the above equations reduce to a linear system, the unknowns of which are the variables q_{ik} and Φ_{ik}.

The response of the fuselage due to an excitation at frequency ω is then a set of sinusoidal oscillations at frequency $|\omega+k\Omega|$, k taking all the integer values between $\pm k_{max}$.

Random excitation : In order to simulate the response to a white noise excitation, the different amplitudes of vibration calculated are summed for a wide range of excitation frequencies.

The spectra of the 3 components of the hub reaction generated by the random excitation between 1 and 40 Hz are shown in fig 3, together with the frequencies calculated in table 2. They correlate

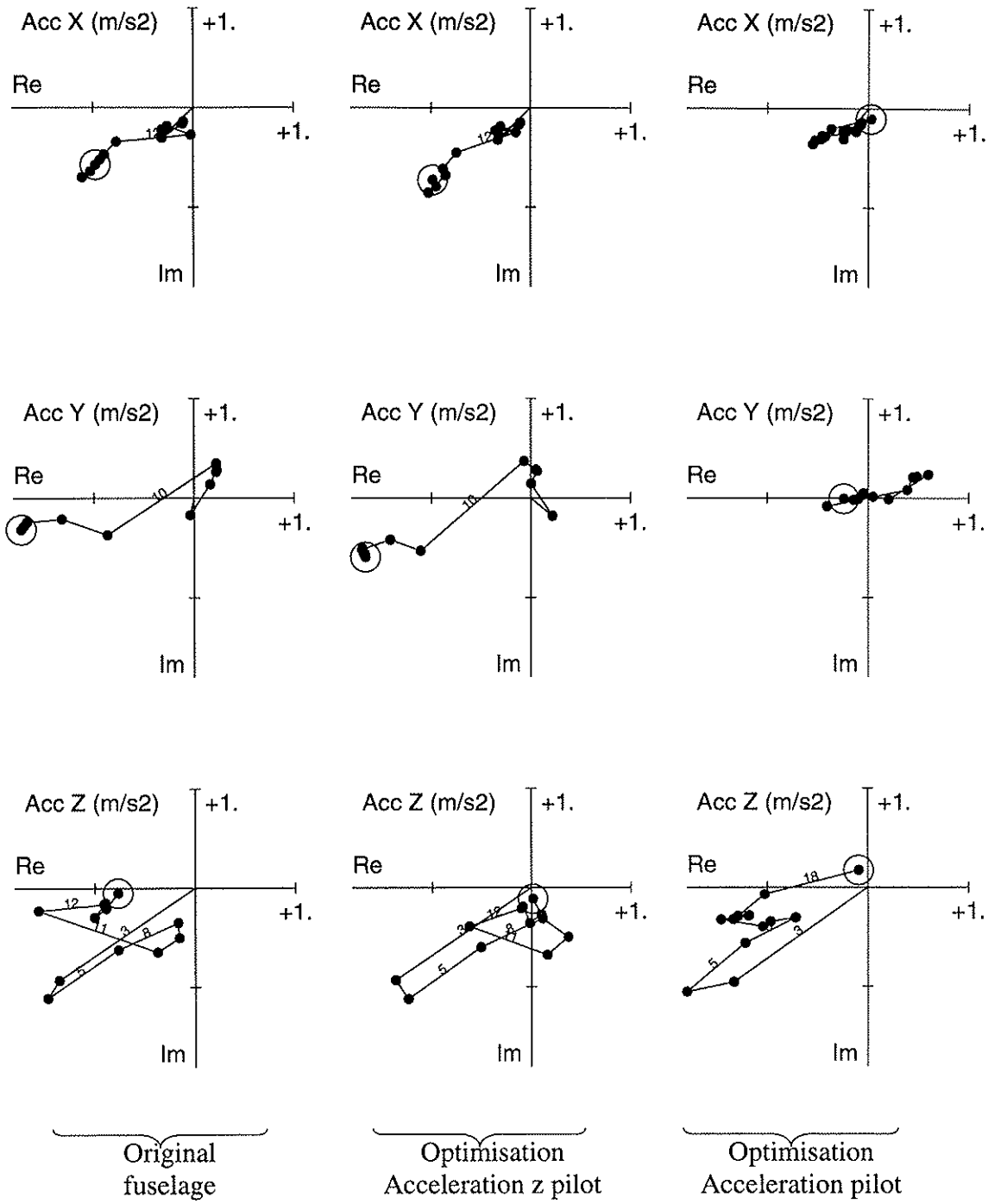

Fig 4: Acceleration at the pilot's seat

well with the different resonance peaks observed.

The fuselage modes (f1, f2, f3, f4, f5, f7) excited by the fin can be seen together with the blade lead-lag (ll1 and ll2).

It would normally not be logical to obtain such a large response in blade lead-lag. In this exercise, lateral movements of the fin are strongly coupled with blade lead-lag because the calculation fixes the rotation speed of the rotor and thus any movement in yaw is directly transferred to the rotor. In a real aircraft, the two would be coupled

through the stiffness and damping of the transmission and much of it would be filtered out.

In addition to the mode resonances, secondary peaks can be observed, (named f1', f3', f4', etc, the prime here stands for a component of a mode at its frequency plus or minus 3Ω, a component which is generated by the periodic coefficients on the fuselage at 3Ω).

Other resonances are due to the blade's progressive (noted ll1+ and ll2+) and regressive modes (noted ll1- and ll2-). As already discussed these modes are not separated by exactly Ω.

It should be kept in mind that the total in-flight hub reaction is the sum of these spectra and of the discrete peaks at nΩ of the in-flight forced response vibration.

6. VIBRATION MINIMISATION

6.1 Introduction

As the ultimate objective is not only to predict vibration levels but also to reduce them, two simple optimisation exercises were undertaken : minimising the z acceleration at the pilot's seat, then the overall pilot's seat acceleration.

Minimisation needs the relaxation of some parameters. As a first step, it is not practical to isolate parameters relative to the fuselage geometry or to mechanical properties, although this will be done in the future. The object of the present exercise is simply to test if some gain can be achieved by tuning the fuselage. Thus a very simple approach has been chosen : the fuselage mode shapes were supposed constant, but their frequencies were used as the variable parameters. The mode shapes may effectively not be too dependant on the fuselage characteristics. The drawback of such a procedure is that it may lead to a stiffening of certain modes which is inconsistent with the softening of others.

Nevertheless, this analysis is of interest as it evaluates the sensitivity of fuselage vibration levels to natural frequencies.

6.2 Procedure

Fuselage modes in table 4 are labelled 7 to 18, the numbers 1 to 6 being reserved for the rigid body degrees of freedom on which no optimisation is possible. The non-rigid mode frequencies were left free to move within plus or minus 20% of their original values.

In order to study the general vibration of the helicopter, the resulting acceleration of the pilot's seat in the three coordinate directions at the frequency 3Ω is reported in fig 4. The circled points represent the amplitude and phase resulting of optimised vibration level in the complex plane. The vibration is decomposed into 18 vectors (ordered from the first to the last) which correspond to the contribution of each fuselage mode. The larger contributions have their mode number noted in the figure.

All the vibration parameters of the helicopter are also shown in table 3-D.

6.3 Minimisation of the z accelerationof the pilot's seat

The optimum set of fuselage frequencies is reported in table 4. The minimum of the vertical acceleration of the pilot's seat has been obtained with a small variation in the frequencies of the 4 fuselage modes which are in the neighbourhood of 3Ω (modes 11 to14).

Fig 4 shows that the general vibration of the helicopter is not changed and that the small shifts in frequency are sufficient to close the z vibration vector and bring it to a near zero value.

6.4 Minimisation of the overall pilot's seat acceleration

Table 4 shows that the optimizer acts here on all the modes and nearly all of them are pushed up toward the 20% limit allowed. This modified fuselage may be very difficult to build.

However, the result is very attractive. Accelerations are greatly reduced, especially in the x and y directions. On the average the fuselage components of vibration are reduced and table 3d shows that the acceleration derivatives in the x and y directions are also considerably reduced which ensures a low vibratory level in the entire helicopter cabin.

Except for mode 16, the low vibratory level was obtained by pushing the frequency away from the 3Ω excitation, which is not too surprising.

Mode 18, which has the highest frequency introduced in the calculation, is still present with quite an large component. Therefore the response obtained may be somewhat different if more modes were used.

As in the z acceleration minimisation, the lateral hub load at 3Ω is doubled.

6.5 Conclusion

The first minimisation shows that little change in the fuselage mechanical properties can bring a local improvement.

The second minimisation shows that a much improved vibratory level can be obtained with greater structural changes, without any apparent penalty. However, the new fuselage thus defined may be unrealistic and more research is needed.

7. CONCLUSIONS

The present study of the vibrations of a complete helicopter required the development of a methodology where an aeroelastic rotor code is coupled with fuselage modes. Resolving this system poses difficult computational problems. Nevertheless, calculations for a simplified helicopter lead to the following general conclusions :

- the flexural modes of the fuselage have a large influence on rotor hub reactions and on fuselage vibrations;
- the analysis of the overall aircraft modes shows that the snapshot eigenvalue method gives a good insight into the modal characteristics. However, a reliable Floquet analysis would be an useful and more accurate tool;
- forced excitation of the fuselage shows that significant response on the hub and blades can be expected;
- first attempt at minimising helicopter cabin vibrations through the tuning of fuselage modal characteristics give very promising results.

Flight test measurements are now required to validate the codes and the methodology used. Studies of realistic optimisation procedures of helicopter vibrations will then be undertaken with direct action on fuselage structural properties.

REFERENCES

1 - D. Petot - *Differential Equation Modelling of Dynamic Stall* - La Recherche Aérospatiale no 5, September 89. (If interested, please ask the author for an errata page for this paper...).

2 - V.K. Truong - *Prediction of Helicopter Airloads Based on Physical Modelling of 3D Unsteady Aerodynamics* - 22nd European Rotorcraft Forum, Brighton, September 96.

3 - F. Quétin - *Recalage de modèles éléments finis en dynamique des structures* - Thesis from the Ecole Nationale Supérieure des Arts et Métiers, 1994.

4 - G. Arnaud, P. Beaumier - *Validation of R85 / METAR on the PUMA RAE Flight Tests* - 18th European Rotorcraft Forum, Avignon, September 92.

5 - D. Petot, J. Bessone - *Numerical Calculation of Helicopter Equations and Comparaison with Experiment* - 18th European Rotorcraft Forum, Avignon, September 92.

6 - J. Bessone, D. Petot - *Calculs du Comportement Aéroélastique des Rotors Comparés à l'Expérience* - La Recherche Aérospatiale, 1994.

7 - J. Bessone, D. Petot - *Evaluation de modèles aérodynamiques et dynamiques des rotors d'hélicoptères par confrontation à l'expérience* - AGARD, Berlin, October 94.

8- P.T.W. Juggins - *A comprehensive approach to coupled rotor-fuselage dynamics* - Forum proocedings of the 14th European Rotorcraft Forum, Paper No. 48, September 1988.